

# Near-Field Robust Adaptive Beamforming Based on Worst-Case Performance Optimization

Jing-ran Lin, Qi-cong Peng, and Huai-zong Shao

**Abstract**—The performance of adaptive beamforming degrades substantially in the presence of steering vector mismatches. This degradation is especially severe in the near-field, for the 3-dimensional source location is more difficult to estimate than the 2-dimensional direction of arrival in far-field cases. As a solution, a novel approach of near-field robust adaptive beamforming (RABF) is proposed in this paper. It is a natural extension of the traditional far-field RABF and belongs to the class of diagonal loading approaches, with the loading level determined based on worst-case performance optimization. However, different from the methods solving the optimal loading by iteration, it suggests here a simple closed-form solution after some approximations, and consequently, the optimal weight vector can be expressed in a closed form. Besides simplicity and low computational cost, the proposed approach reveals how different factors affect the optimal loading as well as the weight vector. Its excellent performance in the near-field is confirmed via a number of numerical examples.

**Keywords**—Robust adaptive beamforming (RABF), near-field, steering vector mismatches, diagonal loading, worst-case performance optimization.

## I. INTRODUCTION

ADAPTIVE beamforming is a ubiquitous task in array signal processing with applications in radar, sonar, acoustics and communications [1], [2]. Its performance, however, degrades dramatically in the presence of steering vector mismatches, for the beamformer tends to misinterpret the desired source as an interference and suppress it (signal self-nulling) [2]. So far many approaches, referred to as robust adaptive beamforming (RABF), have been proposed to improve its performance [2]-[14]. Unfortunately, most existing approaches [5]-[14] deal with the far-field case only and little research has been reported about RABF in the near-field. In applications where the sources are close to the array, however, the far-field assumptions are no longer valid and a more general near-field array model should be turned to, i.e., spherical wavefronts (instead of planar wavefronts) and signal attenuation should be taken into account [3], [4]. In this paper,

the problem of near-field RABF is investigated and a novel approach is proposed. It is a natural extension of the traditional far-field RABF and belongs to the class of diagonal loading approaches.

Diagonal loading [2], [5]-[11], is one of the most popular approaches to improve a beamformer's robustness against steering vector mismatches. On the other hand, how to select the loading level remains an open question in this field. The recently proposed RABF based on worst-case performance optimization, referred to as the worst-case RABF (W-RABF), determines the optimal loading by defining the so-called steering vector uncertainty set and optimizing the worst-case performance [5]-[9]. However, for W-RABF, the optimal loading is solved mainly by iteration at present [5]-[9] and so far no analytical solution has been reported. In this paper, a simple closed-form solution to the optimal loading of the near-field W-RABF is suggested after some approximations and then the optimal weight vector can be expressed in a closed form. Besides its simplicity and low computational cost, the analytical solution reveals how different factors affect the optimal loading and the weight vector.

Although the near-field beamforming often arises in broadband applications (e.g., microphone arrays in small rooms and automobiles), the research in this paper focuses on the narrowband scenario for the sake of simplicity and length constraints. Further studies of the near-field broadband RABF will be addressed in our next work.

## II. NEAR-FIELD ARRAY MODEL

Consider an array of  $M$  sensors and define the reference

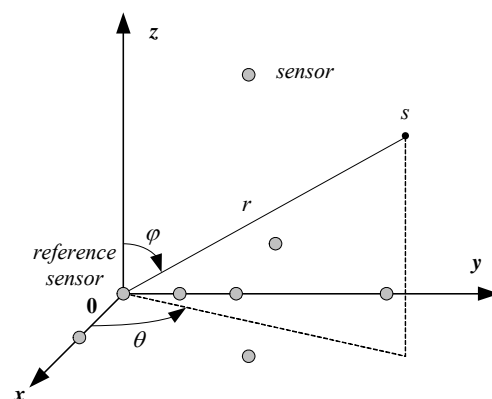


Fig. 1 near-field array model

Manuscript received May 25, 2006. This work was supported in part by the Science and Technology Foundation of Sichuan Province, China, under Grant No. 04GG21-020-20.

Jing-ran Lin, Qi-cong Peng and Huai-zong Shao are with the UESTC-TI DSP Center, School of Communication and Information Engineering (SCIE), University of Electronic Science and Technology of China (UESTC), Chengdu, Sichuan, China (phone: +86-028-83201455; e-mail: jingranlin@163.com, qpeng@uestc.edu.cn and hzshao@uestc.edu.cn).

sensor as the original of a 3-dimensional space, as illustrated in Fig. 1. For an array of length  $L$ , a source is considered to be in the near-field if  $r < 2L^2/\kappa$ , where  $r$  is the distance to the source and  $\kappa$  is the wavelength.

The position vector of a source in direction  $(\theta, \varphi)$ , at distance  $r$  from the reference sensor is denoted as

$$\mathbf{p}_s = r[\mathbf{x}_o, \mathbf{y}_o, \mathbf{z}_o][\cos\theta\sin\varphi, \sin\theta\sin\varphi, \cos\varphi]^T \quad (1)$$

with  $\mathbf{x}_o, \mathbf{y}_o$  and  $\mathbf{z}_o$  the unit-vector of  $x$  axis,  $y$  axis and  $z$  axis, respectively. The sensor position vectors, denoted as  $\mathbf{p}_m, m = 1, 2, \dots, M$ , are similarly defined. Then the distance between the source and the  $m^{\text{th}}$  sensor is,

$$d_m = \|\mathbf{p}_s - \mathbf{p}_m\|, \quad m = 1, 2, \dots, M \quad (2)$$

with  $\|\cdot\|$  the Euclidean vector norm.

Now define the near-field steering vector for a source at distance  $r$  and direction  $(\theta, \varphi)$  as

$$\mathbf{a}(r, \theta, \varphi) = [\alpha_1 e^{-j\psi_1}, \alpha_2 e^{-j\psi_2}, \dots, \alpha_M e^{-j\psi_M}]^T \quad (3)$$

where  $\alpha_m = d_1/d_m$ ,  $\psi_m = 2\pi f(d_m - d_1)/c$ ,  $m = 1, 2, \dots, M$ , are the attenuation factor and phase delay at the  $m^{\text{th}}$  sensor, respectively, with  $f$  and  $c$  the frequency and propagation speed of the source, respectively.

The covariance matrix of array received data, i.e.,  $\mathbf{R}$ , can be described as

$$\mathbf{R} = \sigma_s^2 \mathbf{a} \mathbf{a}^H + \sum_{k=1}^K \sigma_{Jk}^2 \mathbf{a}_{Jk} \mathbf{a}_{Jk}^H + \sigma_n^2 \mathbf{I} = \sigma_s^2 \mathbf{a} \mathbf{a}^H + \mathbf{J} \quad (4)$$

where  $\sigma_s^2$  and  $\sigma_{Jk}^2, k = 1, 2, \dots, K$ , are the powers of the desired source and the  $K$  uncorrelated interferences, respectively,  $\mathbf{a}$  and  $\mathbf{a}_{Jk} \in \mathbb{C}^{M \times 1}, k = 1, 2, \dots, K$ , denote the corresponding near-field steering vectors with the parameters of  $r, \theta$  and  $\varphi$  omitted here for brevity,  $\sigma_n^2$  is the power of the spatially white noise,  $\mathbf{J}$  is the interference-plus-noise matrix and  $(\cdot)^H$  stands for the complex conjugate transpose. In practice,  $\mathbf{R}$  is approximated by

$$\mathbf{R} \approx \frac{1}{N} \sum_{n=1}^N \mathbf{x}(n) \mathbf{x}^H(n) \quad (5)$$

with  $N$  the snapshots number and  $\mathbf{x}(n) \in \mathbb{C}^{M \times 1}$  the array output vector at time index  $n$ .

The near-field adaptive beamforming is typically achieved by

$$\min_{\mathbf{w}} \mathbf{w}^H \mathbf{R} \mathbf{w} \quad s.t. \quad \mathbf{w}^H \mathbf{a} = 1 \quad (6)$$

with  $\mathbf{w} \in \mathbb{C}^{M \times 1}$  the weight vector. And the optimal solution to (6) is [1], [2]

$$\mathbf{w}_o = \frac{\mathbf{R}^{-1} \mathbf{a}}{\mathbf{a}^H \mathbf{R}^{-1} \mathbf{a}} \quad (7)$$

### III. NEAR-FIELD ROBUST ADAPTIVE BEAMFORMING

The performance of the near-field adaptive beamforming of (6) is excellent when  $\mathbf{a}$  is precisely known. However, in many practical situations only the presumed value of  $\mathbf{a}$ , i.e.,  $\tilde{\mathbf{a}}$ , is available and its performance degrades dramatically in the case of steering vector mismatches (namely  $\mathbf{a} \neq \tilde{\mathbf{a}}$ ) [2]. So far many approaches called RABF have been proposed, dealing with the

far-field case mainly [2], [5]-[14]. In this paper, the far-field RABF is extended to near-field scenarios by using the near-field array model of (3), i.e.,

$$\min_{\mathbf{w}} \mathbf{w}^H \mathbf{R} \mathbf{w} \quad s.t. \quad |\mathbf{w}^H \mathbf{c}| \geq 1 \text{ for } \|\mathbf{c} - \tilde{\mathbf{a}}\|^2 \leq \varepsilon^2 \quad (8)$$

with  $\tilde{\mathbf{a}}$  the estimate of the near-field steering vector  $\mathbf{a}$  and  $\varepsilon$  the steering vector distortion bound with  $\|\tilde{\mathbf{a}}\|^2 > \varepsilon^2$  usually.

Apply worst-case performance optimization to (8) and it follows

$$\min_{\mathbf{w}} \mathbf{w}^H \mathbf{R} \mathbf{w} \quad s.t. \quad \min_{\|\mathbf{c} - \tilde{\mathbf{a}}\|^2 \leq \varepsilon^2} |\mathbf{w}^H \mathbf{c}| \geq 1 \quad (9)$$

and it is equivalent to [6], [7]

$$\min_{\mathbf{w}} \mathbf{w}^H \mathbf{R} \mathbf{w} \quad s.t. \quad \mathbf{w}^H \tilde{\mathbf{a}} = \varepsilon \|\mathbf{w}\| + 1 \quad (10)$$

$$\text{Im}\{\mathbf{w}^H \tilde{\mathbf{a}}\} = 0$$

Utilizing the Lagrange's method, the optimal weight vector is

$$\mathbf{w}_o = \frac{\lambda}{\lambda \tilde{\mathbf{a}}^H (\mathbf{R} + \lambda \mathbf{I})^{-1} \tilde{\mathbf{a}} - \varepsilon^2} (\mathbf{R} + \lambda \mathbf{I})^{-1} \tilde{\mathbf{a}} \quad (11)$$

Obviously it belongs to the class of diagonal loading approaches with  $\lambda$  the loading level. In (11) only the parameter of  $\lambda$  is unknown and an approximate closed-form solution will be suggested in the next section.

### IV. OPTIMAL LOADING OF NEAR-FIELD RABF

The optimal loading  $\lambda_o$  of the near-field RABF based on worst-case performance optimization can be determined by inserting (11) into the constraints of (10), i.e., solving

$$(\mathbf{w}_o^H \tilde{\mathbf{a}} - 1)^2 = \varepsilon^2 \|\mathbf{w}_o\|^2 \quad (12)$$

However, this task is by no means easy. Many existing methods solve it by iteration, e.g., the SOCP (second-order cone program) method in [5], [6] and the Newton's method in [7]-[9]. But slow convergence or nonconvergence may occur in iterative methods. Moreover, the solutions by iteration help little in exploiting the relationship between  $\lambda_o$  and such factors as  $\varepsilon, \sigma_n^2, \sigma_s^2$ , etc. Here a simple closed-form solution to  $\lambda_o$  is derived after some approximations, revealing how different factors affect it.

Using the results of (4) and applying the matrix inverse lemma, it follows,

$$(\mathbf{R} + \lambda \mathbf{I})^{-1} = (\mathbf{J} + \lambda \mathbf{I})^{-1} \left[ \mathbf{I} - \frac{\sigma_s^2 \mathbf{a} \mathbf{a}^H (\mathbf{J} + \lambda \mathbf{I})^{-1}}{1 + \sigma_s^2 \mathbf{a}^H (\mathbf{J} + \lambda \mathbf{I})^{-1} \mathbf{a}} \right] \quad (13)$$

Take the eigen-decomposition of  $\mathbf{J}$  as

$$\mathbf{J} = \mathbf{V} \mathbf{\Gamma} \mathbf{V}^H = \mathbf{V}_J \mathbf{\Gamma}_J \mathbf{V}_J^H + \sigma_n^2 \mathbf{V}_n \mathbf{V}_n^H \quad (14)$$

where  $\mathbf{\Gamma} = \text{diag}\{\gamma_1, \gamma_2, \dots, \gamma_M\}$  is the diagonal eigenvalue matrix of  $\mathbf{J}$  with the eigenvalues arranged in decreasing order, i.e.,  $\gamma_1 > \gamma_2 > \dots > \gamma_K > \gamma_{(K+1)} = \gamma_{(K+2)} = \dots = \gamma_M = \sigma_n^2$ ,  $\mathbf{V} = [\mathbf{v}_1, \mathbf{v}_2, \dots, \mathbf{v}_M]$  with  $\mathbf{v}_m \in \mathbb{C}^{M \times 1}$  the eigenvector corresponding to  $\gamma_m, m = 1, 2, \dots, M$ , respectively,  $\mathbf{\Gamma}_J = \text{diag}\{\gamma_1, \gamma_2, \dots, \gamma_K\}$ ,  $\mathbf{V}_J = [\mathbf{v}_1, \mathbf{v}_2, \dots, \mathbf{v}_K]$ ,  $\mathbf{V}_n = [\mathbf{v}_{(K+1)}, \mathbf{v}_{(K+2)}, \dots, \mathbf{v}_M]$ .

Assume that the  $K$  interferences are outside the main beam of

the array to the desired source (the projection of the desired source steering vector onto the interference subspace of  $\mathbf{J}$  is small). Further assume the powers of interferences are large compared with that of the spatial noise ( $\gamma_k \gg \sigma_n^2$ ,  $k = 1, 2, \dots, K$ ). It follows that [10] for  $k = 1, 2, \dots, K$  and  $t = (K+1), (K+2), \dots, M$ ,

$$\frac{|\mathbf{v}_k^H \mathbf{a}|^2}{\gamma_k} \ll \frac{|\mathbf{v}_t^H \mathbf{a}|^2}{\gamma_t}, \quad \frac{|\mathbf{v}_k^H \tilde{\mathbf{a}}|^2}{\gamma_k} \ll \frac{|\mathbf{v}_t^H \tilde{\mathbf{a}}|^2}{\gamma_t} \quad (15)$$

Then

$$\mathbf{a}^H (\mathbf{J} + \lambda \mathbf{I})^{-p} \mathbf{a} = \sum_{m=1}^M \frac{|\mathbf{v}_m^H \mathbf{a}|^2}{(\gamma_m + \lambda)^p} \quad (16)$$

$$\square \sum_{m=K+1}^M \frac{|\mathbf{v}_m^H \mathbf{a}|^2}{(\gamma_m + \lambda)^p} = \frac{\|\mathbf{a}_n\|^2}{(\sigma_n^2 + \lambda)^p}$$

with  $\mathbf{a}_n = [\mathbf{v}_{(K+1)}, \mathbf{v}_{(K+2)}, \dots, \mathbf{v}_M]^H \mathbf{a} = \mathbf{V}_n^H \mathbf{a}$ ,  $\|\mathbf{a}_n\|^2 = \mathbf{a}_n^H \mathbf{a}_n$  and  $p$  a positive integer. Similarly,

$$\mathbf{a}^H (\mathbf{J} + \lambda \mathbf{I})^{-p} \tilde{\mathbf{a}} \approx \frac{\mathbf{a}_n^H \tilde{\mathbf{a}}_n}{(\sigma_n^2 + \lambda)^p} \quad (17)$$

with  $\tilde{\mathbf{a}}_n = [\mathbf{v}_{(K+1)}, \mathbf{v}_{(K+2)}, \dots, \mathbf{v}_M]^H \tilde{\mathbf{a}}$ .

Inserting (16), (17) into (13) and the latter into (12), after some direct derivations, it follows

$$\|\tilde{\mathbf{a}}_n\|^2 - 2L \left| \mathbf{a}_n^H \tilde{\mathbf{a}}_n \right|^2 + L^2 \left| \mathbf{a}_n^H \tilde{\mathbf{a}}_n \right|^2 \|\mathbf{a}_n\|^2 = \left( \frac{\lambda + \sigma_n^2}{\lambda \varepsilon^{-1}} \right)^2 \quad (18)$$

with  $L = (\lambda + \sigma_n^2 + \sigma_s^2 \|\mathbf{a}_n\|^2)^{-1} \sigma_s^2$ .

Let  $\mathbf{a}_n = \tilde{\mathbf{a}}_n + \Delta_n$  and  $\|\Delta_n\|^2$  is negligible compared with  $\|\mathbf{a}_n\|^2$  or  $\|\tilde{\mathbf{a}}_n\|^2$  when the steering vector error is small, i.e.,  $\|\mathbf{a}_n\|^2 \approx \|\tilde{\mathbf{a}}_n\|^2$ . Then,

$$\begin{aligned} \left| \mathbf{a}_n^H \tilde{\mathbf{a}}_n \right|^2 &= \tilde{\mathbf{a}}_n^H \mathbf{a}_n \mathbf{a}_n^H \tilde{\mathbf{a}}_n = \tilde{\mathbf{a}}_n^H (\tilde{\mathbf{a}}_n + \Delta_n) \mathbf{a}_n^H (\mathbf{a}_n - \Delta_n) \\ &= \|\tilde{\mathbf{a}}_n\|^2 \|\mathbf{a}_n\|^2 + \|\mathbf{a}_n\|^2 \tilde{\mathbf{a}}_n^H \Delta_n - \|\tilde{\mathbf{a}}_n\|^2 \mathbf{a}_n^H \Delta_n - \tilde{\mathbf{a}}_n^H \Delta_n \mathbf{a}_n^H \Delta_n \quad (19) \\ &\approx \|\tilde{\mathbf{a}}_n\|^2 \|\mathbf{a}_n\|^2 - \|\mathbf{a}_n\|^2 \Delta_n^H \Delta_n - \tilde{\mathbf{a}}_n^H \Delta_n \mathbf{a}_n^H \Delta_n \end{aligned}$$

Eliminating the second-order terms of  $\Delta_n$  in (19), it turns out

$$\left| \mathbf{a}_n^H \tilde{\mathbf{a}}_n \right|^2 \approx \|\tilde{\mathbf{a}}_n\|^2 \|\mathbf{a}_n\|^2 \quad (20)$$

This approximation is reasonable because: Firstly, RABF can no longer compensate for the steering vector mismatch when it exceeds a specific threshold [11]; Secondly, the larger the distortion bound  $\varepsilon$  is, the poorer capability RABF will possess in rejecting interferences adaptively [2], [8]. In a word, it is just for small or middle  $\varepsilon$  that the use of RABF is advisable. Inserting (20) into (18), the latter can be simplified as

$$\left( \frac{\|\tilde{\mathbf{a}}_n\|}{\lambda + \sigma_n^2 + \sigma_s^2 \|\mathbf{a}_n\|^2} \right)^2 = \left( \frac{\varepsilon}{\lambda} \right)^2 \quad (21)$$

From (21) two simple closed-form solution to  $\lambda$  can be easily found, i.e.,

$$\lambda_1 = \frac{\varepsilon(\sigma_n^2 + \sigma_s^2 \|\mathbf{a}_n\|^2)}{\|\tilde{\mathbf{a}}_n\| - \varepsilon}, \quad \lambda_2 = \frac{-\varepsilon(\sigma_n^2 + \sigma_s^2 \|\mathbf{a}_n\|^2)}{\|\tilde{\mathbf{a}}_n\| + \varepsilon} \quad (22)$$

Obviously  $\lambda_1 > 0$  and  $\lambda_2 < 0$ . It can be proven that the negative roots of (12), if any, do not satisfy the constraint of  $\mathbf{w}_o^H \tilde{\mathbf{a}} > 1$ , which is required by (10) implicitly (see the appendix for detail). Therefore, the optimal loading of the near-field RABF based on worst-case performance optimization is

$$\lambda_o = \frac{\varepsilon(\sigma_n^2 + \sigma_s^2 \|\mathbf{a}_n\|^2)}{\|\tilde{\mathbf{a}}_n\| - \varepsilon} \approx \frac{\varepsilon(\sigma_n^2 + \sigma_s^2 \|\tilde{\mathbf{a}}_n\|^2)}{\|\tilde{\mathbf{a}}_n\| - \varepsilon} \quad (23)$$

and consequently the optimal weight vector can be expressed in a closed-form as

$$\mathbf{w}_o = \frac{\lambda_o}{\lambda_o \tilde{\mathbf{a}}^H (\mathbf{R} + \lambda_o \mathbf{I})^{-1} \tilde{\mathbf{a}} - \varepsilon^2} (\mathbf{R} + \lambda_o \mathbf{I})^{-1} \tilde{\mathbf{a}} \quad (24)$$

with  $\lambda_o$  given in (23).

Observing the results in (23) and (24), the following points are straightforward. Firstly, the optimal loading level  $\lambda_o$  depends on the noise level  $\sigma_n^2$ , the desired source power  $\sigma_s^2$ , the steering vector distortion bound  $\varepsilon$  and the norm of the steering vector projection onto the subspace orthogonal to the interference subspace, i.e.,  $\|\mathbf{a}_n\|^2$  and  $\|\tilde{\mathbf{a}}_n\|^2$ .

Secondly,  $\lambda_o$  increases as  $\varepsilon$  or  $\sigma_s^2$  increases. When  $\varepsilon$  approaches  $\|\tilde{\mathbf{a}}_n\|$ , an infinite loading is required. Consequently the RABF turns to the data-independent beamforming and no capability of rejecting interferences adaptively is achieved. On the other hand, when  $\varepsilon$  decreases to zero,  $\lambda_o$  approaches zero asymptotically and then the RABF turns to the standard adaptive beamforming (SABF).

Thirdly, since the optimal loading can be computed directly, the computational cost of the proposed method is the same as that of SABF, requiring  $O(M^2)$  flops. It is computationally more efficient than the iterative methods. For example, the SOCP developed requires  $O(\rho M^3)$  flops with  $\rho$  the number of iterations. The Newton's method, although less computational demanding than the SOCP developed, consumes at least  $100M$  flops more than the proposed one. Moreover, the two iterative methods provide little information about how different factors affect the optimal loading and the weight vector.

## V. NUMERICAL EXAMPLES

Consider a uniform linear array with  $M = 10$  sensors along with the  $y$  axis in Fig. 1. The wavelength of the desired source is  $\kappa = 0.34m$  and the sensors are spaced half wavelength apart, i.e.,  $0.17m$ . Then the source should be considered as a near-field one if it is within the region of  $r < 14m$ .

Three narrowband near-field uncorrelated signals impinge upon the array: the desired source from  $(r_s, \theta_s, \varphi_s) = (6m, 90^\circ, 0^\circ)$ , two interferences from  $(r_{J1}, \theta_{J1}, \varphi_{J1}) = (5m, 90^\circ, -20^\circ)$  and  $(r_{J2}, \theta_{J2}, \varphi_{J2}) = (5m, 90^\circ, 30^\circ)$ , respectively. The level of the spatially white Gaussian noise is  $0dB$ , i.e.,  $\sigma_n^2 = 1$ . The desired source power is  $10dB$ , and the powers of the two interferences are both  $30dB$ . Assume the estimate of the desired source position is  $(r, \theta, \varphi) = (6.5m, 90^\circ, 2^\circ)$  and consequently  $\varepsilon = 1.6995$ .

Four algorithms are involved in the following simulations: (1) the near-field SABF (N-SABF); (2) the near-field RABF with a fixed loading (FL) of  $10dB$  above the noise level (NFL-RABF);

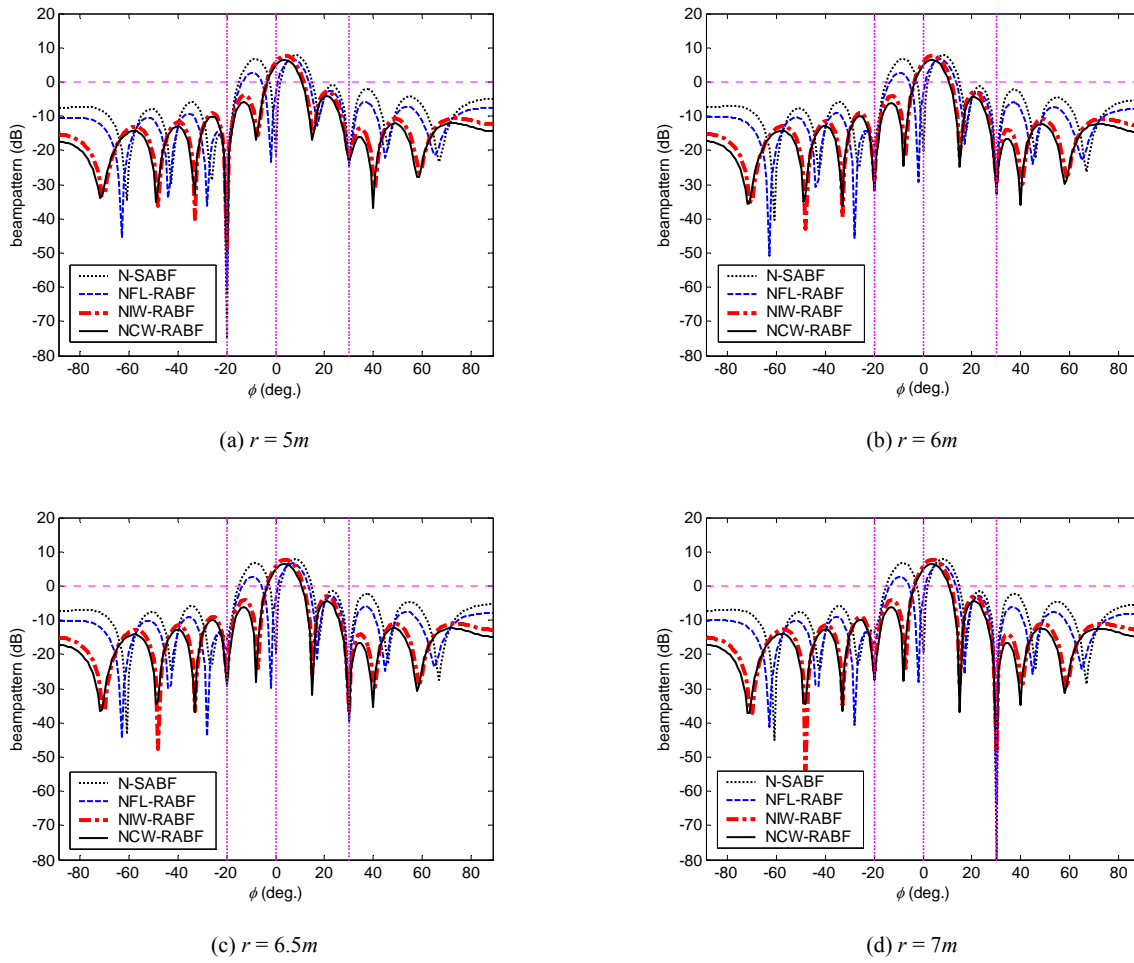


Fig. 2 beampattern comparison of the four algorithms with (a)  $r = 5m$ ; (b)  $r = 6m$ ; (c)  $r = 6.5m$ ; (d)  $r = 7m$

(3) the near-field RABF based on worst-case performance optimization with the loading solved by iteration, i.e., the near-field iterative worst-case RABF (NIW-RABF); (4) the proposed method, i.e., the near-field closed-form worst-case RABF (NCW-RABF) with the optimal loading and weight vector solved by (23) and (24), respectively. In this paper, the signal to interference plus noise ratio (SINR) is used to measure the performance of a beamformer, which is computed as

$$\text{SINR} = \frac{\sigma_s^2 |\mathbf{w}_o^H \mathbf{a}|^2}{\mathbf{w}_o^H \left( \sum_{k=1}^K \sigma_{Jk}^2 \mathbf{a}_{Jk} \mathbf{a}_{Jk}^H + \sigma_n^2 \mathbf{I} \right) \mathbf{w}_o} = \frac{\sigma_s^2 |\mathbf{w}_o^H \mathbf{a}|^2}{\mathbf{w}_o^H \mathbf{J} \mathbf{w}_o} \quad (25)$$

The beampattern comparisons of the four algorithms at different distance  $r$  are illustrated in Fig. 2. In all the subfigures of Fig. 2, N-SABF works very poorly and suppresses the desired source as an interference. This signal self-nulling is alleviated in NFL-RABF. However, since the 10dB fixed loading is not necessarily optimal, the desired source is still

suppressed somewhat. On the other hand, the desired source does not suffer from suppression in both NIW-RABF and NCW-RABF. In addition, the beampatterns of NIW-RABF and NCW-RABF are very close to each other, implying (23) approximates the actual optimal loading accurately. Since the near-field array model is used, the effect of distance  $r$  onto the beampattern is observed. In Fig. 2(a), i.e.,  $r = 5m$ , the first interference is suppressed more than in the other three subfigures and in Fig. 2(d), i.e.,  $r = 7m$ , the second interference is suppressed more deeply. The discrimination of distance can be seen clearly in Fig. 3, where the 2-dimensional beampatterns of N-SABF and NCW-SABF are displayed. In Fig. 3(a), N-SABF has deep notches at the positions (not in the directions) of all the three sources (both interferences and the desired source). However, in Fig. 3(b), NCW-RABF only suppresses the interferences, i.e., is robust against steering vector mismatches in the near-field.

The performance comparisons vs. snapshots number  $N$  are illustrated in Fig. 4. The SINR comparison is shown in Fig. 4(a),

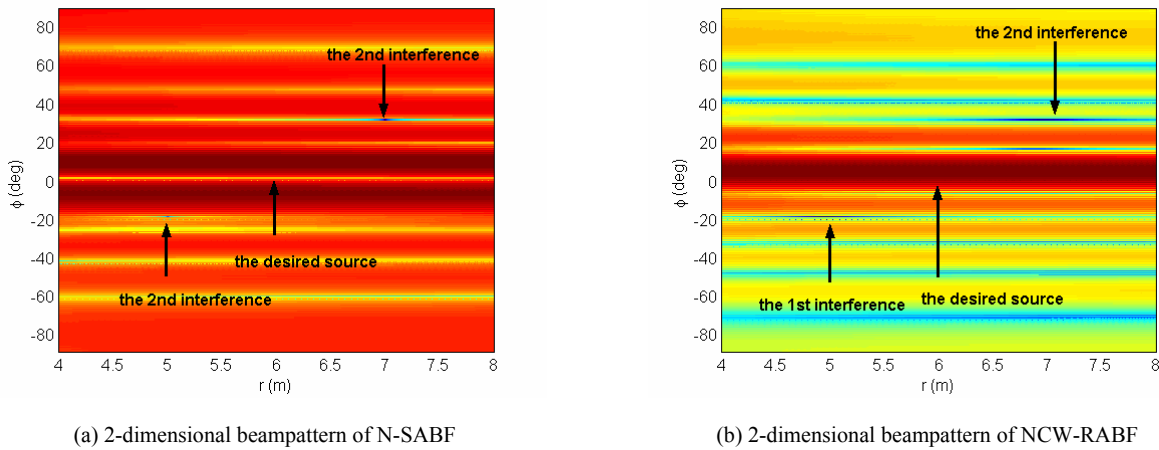
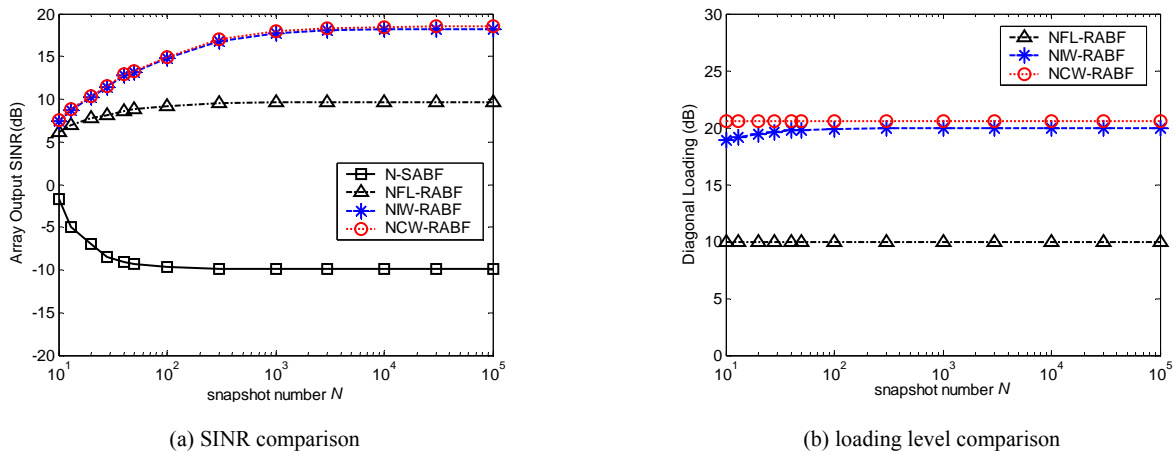


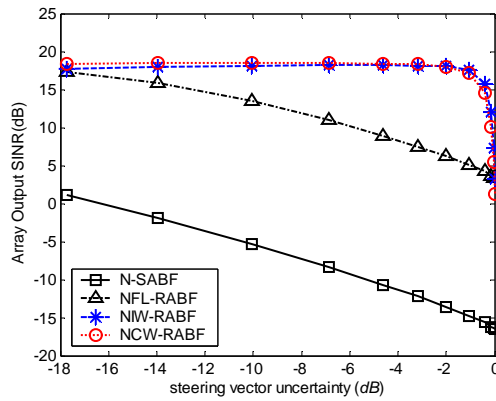
Fig. 3 2-dimensional beampattern comparison with (a) N-SABF; (b) NCW-RABF

Fig. 4 performance comparison vs. snapshots number  $N$  at  $\varepsilon = 1.6995$  with (a) SINR comparison; (b) loading level comparison

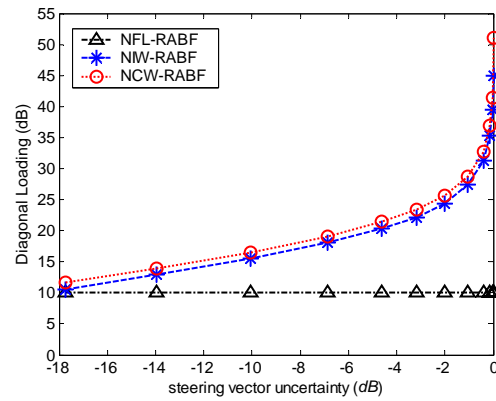
whereas the loading level comparison in Fig. 4(b). At each snapshots number, 100 *Monte Carlo* trials are carried out to get the averaged results. It is obvious in Fig. 4(a) that in the presence of steering vector mismatches, the performance of N-SABF is unacceptable. NFL-RABF offers improved robustness, but its performance is still unsatisfactory since the fixed loading is not optimal necessarily. Both NIW-RABF and NCW-RABF achieve higher SINR than the former two algorithms. Moreover, the results of NIW-RABF and NCW-RABF almost coincide with each other, implying (23) approximates the actual optimal loading very accurately. This is attested in Fig. 4(b) where the optimal loadings solved by (23) are very close to those by iteration.

Change the estimation error of the desired source position and the performance comparisons vs. the steering vector uncertainty are illustrated in Fig. 5 with the snapshots number

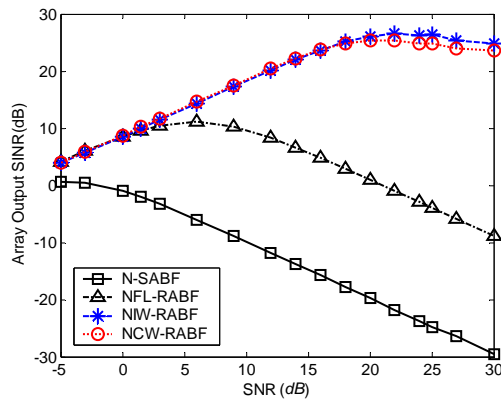
fixed at  $N = 1000$ . Here the steering vector uncertainty is defined as  $Un(dB) = 20\log_{10}(\|\mathbf{a}\|^{-1}\varepsilon)$ . Observing the results in Fig. 5, the following points are straightforward. Firstly, in the presence of even slight steering vector mismatches, N-SABF works very poorly. Secondly, NFL-RABF does improve the robustness. However, its performance is still poor in the case of high steering vector uncertainties. Thirdly, both NIW-RABF and NCW-RABF outperform the former two algorithms. Again the results of the two worst-case RABF are very close to each other and (23) is an accurate approximation to the actual optimal loading. Fourthly, the optimal loading increases when the steering vector uncertainty (or  $\varepsilon$ ) increases, in accordance with the analysis of (23). Fifthly, when the uncertainty is below  $-2dB$ , the SINR of NIW-RABF and NCW-RABF is nearly constant and independent of  $\varepsilon$ . On the other hand, when the uncertainty exceeds this threshold, the performance degrades



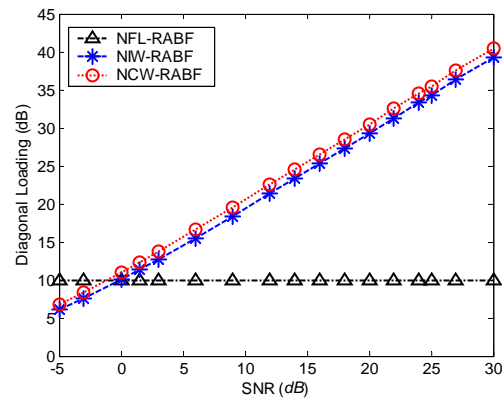
(a) SINR comparison



(b) loading level comparison

Fig. 5 performance comparison vs. the steering uncertainty at  $N = 1000$  with (a) SINR comparison; (b) loading level comparison

(a) SINR comparison



(b) loading level comparison

Fig. 6 performance comparison vs. SNR at  $N = 1000$  and  $\epsilon = 1.6995$  with (a) SINR comparison; (b) loading level comparison

abruptly, for large loading levels cause them act more like data-independent beamformers and lose the adaptive capability of rejecting the interferences.

Change the desired source power  $\sigma_s^2$  and the performance comparisons vs. signal to noise ratio (SNR) are illustrated in Fig. 6 with the snapshots number fixed at  $N = 1000$  and the other parameters the same as in the first simulation. N-SABF works very poorly as expected. The performance of NFL-RABF is scenario dependent. When the input SNR is about  $0\text{dB}$ , the optimal loading of the near-field worst-case RABF is  $10\text{dB}$ , i.e., the same as the fixed loading. Then the SINR of NFL-RABF is the same as those of NIW-RABF and NCW-RABF at this point. However, its performance degrades as the SNR deviates from  $0\text{dB}$  for the  $10\text{dB}$  fixed loading is no longer optimal. On the other hand, NIW-RABF and NCW-RABF achieve better robustness against SNR variation

and it is confirmed again in this simulation that (23) approximates the actual optimal loading accurately. In addition, the optimal loading increases as SNR (or  $\sigma_s^2$ ) increases, in accordance with the analysis of (23).

## VI. CONCLUSION

A novel approach of near-field robust adaptive beamforming (RABF) is proposed in this paper, aiming at robustness against steering vector mismatches in the near-field. It is a natural extension of the traditional far-field RABF and belongs to the class of diagonal loading approaches with the loading level determined based on worst-case performance optimization. However, other than searching for the optimal loading by iteration, the proposed method suggests a simple approximate closed-form solution and then the optimal weight vector can be expressed in a closed-form. Besides its simplicity and low

computational cost, the closed-form solution reveals how different factors affect the optimal loading. For detail, the optimal loading depends on the noise level  $\sigma_n^2$ , the desired source power  $\sigma_s^2$ , the steering vector distortion bound  $\varepsilon$  and the norm of the steering vector projection onto the subspace orthogonal to the interference subspace, i.e.,  $\|\mathbf{a}_n\|^2$  and  $\|\tilde{\mathbf{a}}_n\|^2$ . Moreover, the optimal loading increases as  $\varepsilon$  or  $\sigma_s^2$  increases. Numerical examples confirm that compared with many existing methods in this field, the proposed one offers better robustness against steering vector mismatches in the near-field and achieves the capability of discrimination of distance. It is also confirmed that the proposed closed-form solution is a very accurate approximation to the actual optimal loading.

It should be noted that although the near-field beamforming often arises in broadband cases, the research in this paper is based on the narrowband assumption for the sake of simplicity and length constraints. When broadband sources are concerned, one must consider how to ensure the frequency invariance of the beampattern besides the issues in this paper. And this problem will be addressed in our next work.

#### APPENDIX

It will be proven in the appendix that the optimal loading of the near-field worst-case RABF is unique and positive.

Perform the eigen-decomposition of  $\mathbf{R}$  as

$$\mathbf{R} = \mathbf{U}\mathbf{\Sigma}\mathbf{U}^H = \sum_{m=1}^M \eta_m \mathbf{u}_m \mathbf{u}_m^H \quad (26)$$

with  $\eta_m$  the eigenvalues of  $\mathbf{R}$  arranged in decreasing order and  $\mathbf{u}_m \in \mathbf{C}^{M \times 1}$  the eigenvector associated with  $\eta_m$ ,  $m = 1, 2, \dots, M$ . Since  $\mathbf{R}$  is almost always positive definite in practice, it follows that  $\eta_1 > \eta_2 > \dots > \eta_M > 0$ . It is easy to show (12) is equivalent to

$$f(\lambda) \triangleq \sum_{m=1}^M \frac{\lambda^2 |\theta_m|^2}{(\lambda + \eta_m)^2} = \varepsilon^2 \quad (27)$$

with  $\theta_m = \mathbf{u}_m^H \tilde{\mathbf{a}}$ .

Besides (12) the optimal loading should satisfy the constraint of  $\mathbf{w}_o^H \tilde{\mathbf{a}} > 1$ , which is required by (10) implicitly. This constraint can be written as

$$g(\lambda) \triangleq \sum_{m=1}^M \frac{\lambda |\theta_m|^2}{\lambda + \eta_m} > \varepsilon^2 \quad (28)$$

Consider

$$f(\lambda) - g(\lambda) = - \sum_{m=1}^M \frac{\lambda \eta_m |\theta_m|^2}{(\lambda + \eta_m)^2} \quad (29)$$

Then  $f(\lambda) > g(\lambda)$  for  $\lambda < 0$  and  $f(\lambda) < g(\lambda)$  for  $\lambda > 0$ . Consequently it can be concluded that the negative roots of (12), if any, do not satisfy  $\mathbf{w}_o^H \tilde{\mathbf{a}} > 1$ .

On the other hand, since  $f(0) = 0 < \varepsilon^2$ ,  $f(\infty) = \|\tilde{\mathbf{a}}\|^2 > \varepsilon^2$  and  $f'(\lambda) > 0$  (monotonically increasing) for  $\lambda > 0$ , (12) has a unique root  $\lambda_o$  in the positive semi-axes. Based on the fact that  $f(\lambda) < g(\lambda)$  for  $\lambda > 0$ , i.e.,  $g(\lambda_o) > \varepsilon^2$ , it follows  $\lambda_o$  satisfies  $\mathbf{w}_o^H \tilde{\mathbf{a}} > 1$ .

Therefore, the optimal loading for the near-field worst-case RABF is unique and positive.

#### REFERENCES

- [1] J. Capon, "High resolution frequency-wavenumber spectrum analysis," *Proc. IEEE*, vol. 57, Aug. 1969, pp. 1408-1418.
- [2] H. L. Van Trees, *Detection, Estimation, and Modulation Theory, Part IV, Optimum Array Processing*. New York: Wiley, 2002.
- [3] Y. R. Zheng, R. A. Goubran, and M. El-Tanany, "Robust near-field adaptive beamforming with distance discrimination," *IEEE Trans. Signal Processing*, vol. 12, no. 5, Sep. 2004, pp. 478-488.
- [4] S. Doclo, M. Moonen, "Design a far-field and near-field broadband beamformers using eigenfilters," *Signal Processing*, vol. 83, no. 12, Dec. 2003, pp. 2641-2673.
- [5] A. B. Gershman, "Robust adaptive beamforming: an overview of recent trends and advances in the field," in *Proc. Int. Conf. Antenna Theory and Techniques*, vol. 1, Sept. 2003, pp. 30-35.
- [6] S. A. Vorobyov, A. B. Gershman, and Z. Luo, "Robust adaptive beamforming using worst-case performance optimization: a solution to the signal mismatch problem," *IEEE Trans. Signal Processing*, vol. 51, Feb. 2003, pp. 313-324.
- [7] R. G. Lorenz, S. P. Boyd, "Robust minimum variance beamforming," *IEEE Trans. Signal Processing*, vol. 53, no. 5 May. 2005, pp. 1684-1696.
- [8] J. Li, P. Stoica, Z.-S. Whang, "On robust Capon beamforming and diagonal loading," *IEEE Trans. Signal Processing*, vol. 51, no. 7, July 2003, pp. 1702-1715.
- [9] J. Li, P. Stoica, Z.-S. Wang, "Doubly constrained robust Capon beamformer," *IEEE Trans. Signal Processing*, vol. 52, no. 9, Sept. 2004, pp. 2407-2423.
- [10] F. Vincent, O. Besson, "Steering vector errors and diagonal loading," *IEE Proc. -Radar Sonar Navig.*, vol. 151, no. 6, Dec. 2004, pp. 337-343.
- [11] O. Besson, F. Vincent, "Performance analysis of beamformers using generalized loading of the covariance matrix in the presence of random steering vector errors," *IEEE Trans. Signal processing*, vol. 53, no. 2, Feb. 2005, pp. 452-459.
- [12] D. D. Feldman and L. J. Griffiths, "A projection approach to robust adaptive beamforming," *IEEE Trans. Signal Processing*, vol. 42, April, 1994, pp. 867-876.
- [13] M. H. Er, A. Cantoni, "An alternative formulation for an optimum beamformer with robustness capability," *Proc. Int. Elect. Eng. F, Commun., Radar, Signal Process.*, vol. 132, 1985, pp. 447-460.
- [14] Z. Tian, K. L. Bell, H. L. Van Trees, "A recursive least squares implementation for LCMP beamforming under quadratic constraint," *IEEE Trans. Signal Processing*, vol. 49, no. 6, June, 2001, pp. 1138-1145.

**Jing-ran Lin** was born in Sichuan, China, in Nov. 1978. He received the B.S. degree in computer communication and the M.S. degree in signal processing from University of Electronic Science and Technology of China (UESTC), Chengdu, China, in 2001 and 2004, respectively.

He is now with the UESTC-TI DSP Center and pursuing the Ph.D. degree in signal processing. His research interests include statistical signal processing, array signal processing, adaptive beamforming, parameter estimation and real-time signal processing.